AD-757 657

# DYNAMIC MEASUREMENTS OF DETONATOR OUTPUT

N. L. Coleburn, et al

Naval Ordnance Laboratory
White Oak, Maryland

29 January 1973

DISTRIBUTED BY:

NTIS

National Technical Information Service
U. S. DEPARTMENT OF COMMERCE
5285 Port Royal Road, Springfield Va. 22151

NOLTR 72-266

AD757657

757657

# DYNAMIC MEASUREMENTS OF DETONATOR OUTPUT

By
N. L. Coleburn
T. P. Liddiard
L. A. Roslund

DDC
RECEIVED
MAR 30 1973
C

29 JANUARY 1973

NOL

NAVAL ORDNANCE LABORATORY, WHITE OAK, SILVER SPRING, MARYLAND

NOLTR 72-266

APPROVED FOR PUBLIC RELEASE;
DISTRIBUTION UNLIMITED

Reproduced by
NATIONAL TECHNICAL
INFORMATION SERVICE
U S Department of Commerce
Springfield VA 22151

41 R

UNCLASSIFIED
Security Classification

DOCUMENT CONTROL DATA - R & D

(Security classification of title, body of abstract and indexing annotation must be entered when the overall report is classified)

| | |
|---|---|
| 1. ORIGINATING ACTIVITY (Corporate author) Naval Ordnance Laboratory White Oak, Silver Spring, Maryland 20910 | 2a. REPORT SECURITY CLASSIFICATION UNCLASSIFIED<br>2b. GROUP |

3. REPORT TITLE

DYNAMIC MEASUREMENTS OF DETONATOR OUTPUT

4. DESCRIPTIVE NOTES (Type of report and inclusive dates)

5. AUTHOR(S) (First name, middle initial, last name)

N. L. Coleburn, T. P. Liddiard, and L. A. Roslund

| | | |
|---|---|---|
| 6. REPORT DATE 29 January 1973 | 7a. TOTAL NO. OF PAGES iv + 34 | 7b. NO. OF REFS 1 |
| 8a. CONTRACT OR GRANT NO. | 9a. ORIGINATOR'S REPORT NUMBER(S) NOLTR 72-266 | |
| b. PROJECT NO. Task NOL-591/HDL | 9b. OTHER REPORT NO(S) (Any other numbers that may be assigned this report) | |

10. DISTRIBUTION STATEMENT

Approved for public release; distribution unlimited.

| | |
|---|---|
| 11. SUPPLEMENTARY NOTES | 12. SPONSORING MILITARY ACTIVITY U. S. Army Material Command Harry Diamond Laboratories Washington, D. C. 20438 |

13. ABSTRACT


Various techniques for possible use in evaluating dynamic detonator output were investigated. High-speed cameras were used in detonator test firings to record the motion of detonator fragments, explosion gases, shocks in air and in water, and build-up to detonation in boosters. The M84 detonator fired in air has an initial case expansion velocity of 1560 meters/second and an initial explosion gas expansion velocity of 2620 meters/second. The peak shock pressure transmitted into water by the M84 is 46.2 kilobars. Each evaluation technique offers distinct advantages. However, measurements of underwater shock pressures and booster response appear likely to provide the best level of cost effectiveness.

Measurements of electrical response using the M84 detonator show that reductions in input energy cause increases in functioning time but have no effect on other output parameters until the initiation failure point is reached.


DD FORM 1 NOV 65 1473 (PAGE 1)

S/N 0101-807-6801

UNCLASSIFIED
Security Classification

UNCLASSIFIED
Security Classification

| 14 KEY WORDS | LINK A ROLE | LINK A WT | LINK B ROLE | LINK B WT | LINK C ROLE | LINK C WT |
|---|---|---|---|---|---|---|
| Detonator Output | | | | | | |
| Microdetonator Output | | | | | | |
| Fragment Velocity | | | | | | |
| Detonation Build-up | | | | | | |
| Initiation of Boosters | | | | | | |

DD FORM 1 NOV 65 1473 (BACK)
(PAGE 2)

UNCLASSIFIED
Security Classification

NOLTR 72-266 29 January 1973

DYNAMIC MEASUREMENTS OF DETONATOR OUTPUT

The work described in this report was done under the sponsorship of the U. S. Army Material Command's Harry Diamond Laboratories. The Naval Ordnance Laboratory Task Title was: Detonator Function Test (Task NOL-591/HDL). The objective was to find better ways of determining dynamic detonator output. The attainment of this objective could lead to improved safety and reliability of detonators and explosive trains.

The identification of any commercial product in this report implies neither a criticism nor an endorsement of it by the Naval Ordnance Laboratory.

The authors are indebted to R. K. Warner of the Harry Diamond Laboratories for providing valuable information and guidance for this task.

ROBERT WILLIAMSON II
Captain, USN
Commander

C. J. Aronson

C. J. ARONSON
By direction

CONTENTS

| | | Page |
|---|---|---|
| I. | INTRODUCTION | 1 |
| II. | EXPERIMENTAL | 2 |
| | A. Electrical Characteristics | 2 |
| | B. Detonators Under Water (Aquarium Technique) | 3 |
| | C. Detonators Initiated in Air | 6 |
| | D. Build up to Detonation in Booster Explosives | 9 |
| III. | DISCUSSION AND RECOMMENDATIONS | 12 |
| | A. Electrical Characteristics | 12 |
| | B. Underwater Measurements | 12 |
| | C. Case and Gas Expansion in Air | 14 |
| | D. Detonation Buildup in Booster Explosives | 14 |
| IV. | REFERENCES | 16 |

TABLES

| Table | | |
|---|---|---|
| 1 | Internal Initiation and Functioning Times of the M84 Detonator | 4 |
| 2 | M84 Detonator Case Fragment Velocities in Air | 7 |
| 3 | M84 Detonator Shock Characteristics in Air | 8 |
| 4 | Run-Distance Results for Tetryl Initiated by the Atlas Microdetonator | 11 |
| 5 | Comparison of Detonator Evaluation Experiments | 13 |

ILLUSTRATIONS

| Figure | | |
|---|---|---|
| 1 | M84 Detonator | 17 |
| 2 | Firing Circuit | 18 |
| 3 | Oscillograms of M84 Detonator Electrical Response to a 5-Volt Input Pulse | 19 |
| 4 | Oscillograms of M84 Detonator Electrical Response to a 17-Volt Input Pulse | 20 |
| 5 | The Aquarium Arrangement for Measuring Detonator Output in Water | 21 |

ILLUSTRATIONS (Continued)

| Figure | | Page |
|---|---|---|
| 6 | Smear Camera Shadowgraph of Axial Shock Wave Motion Produced by the M84 Fired Underwater . . . . | 22 |
| 7 | Underwater Shock Wave Velocity Decay . . . . . | 23 |
| 8 | Impedance Match Solution for Peak Pressures Transmitted into Water by the M84 Detonator . . . . | 24 |
| 9 | Smear Camera Record of Lateral Shock Wave Expansion from the M84 Detonator Fired Underwater . . . . . | 25 |
| 10 | Framing Camera Shadowgraphs of Shock Wave and Product Gas Expansion from the M84 Detonator Fired Underwater . . . . . | 26 |
| 11 | Framing Camera Shadowgraphs of Shock Wave Expansion from the M84 Detonator Fired in Air . . . . . | 27 |
| 11A | An Enlarged Frame from Figure 11 . . . . . | 28 |
| 12A | Test Arrangement . . . . . | 29 |
| 12B | Smear Camera Trace of Axial Shock from the M84 Detonator Fired in Air . . . . . | 29 |
| 13 | Smear Camera Record of Lateral Case Expansion from the M84 Detonator Fired in Air . . . . . | 30 |
| 14 | Case Expansion Profile from the M84 Detonator Fired in Air . . . . . | 31 |
| 15A | The Microdetonator/Tetryl-Booster System . . . . . | 32 |
| 15B | The Smear-Camera Trace of the Detonation Along the Booster Surface and the Streaks (Timing Markers) from the Exploding Bridgewire and the Detonator . . . . . | 32 |
| 16 | The Microdetonator . . . . . | 33 |
| 17 | Superposed Sketches of the Detonation Traces from Shots 5, 6, and 8 . . . . . | 34 |

# I. INTRODUCTION

Deviations from uniformity in the manufacturing process of detonators can cause enough variation in the details of energy transfer to affect initiation of explosive trains. If the energy transfer processes are adequately known, the conditions necessary for reliable initiation can be determined. Unfortunately, a detonator's dynamic output is very difficult to measure accurately because the quantity of explosive involved is small, and it is consumed very rapidly. Background discussions of presently used methods to determine detonator and explosive component output and the need for improvements are given in references 1, 2, and 3.*

Usually the output of a detonator or explosive train is checked by means of a dent test. The output is taken to be indicated by the depth of the dent produced in a metal like steel or aluminum. The dent is an end result from which the variation of output with time cannot be deduced. What is needed are accurate measurements of the important parameters involved in the dynamic output of detonators.

The purpose of this work is to investigate various techniques for determining the quantitative dynamic output of detonators. Our approach is to use both smear and framing cameras to record the motion of detonator-case fragments, air shocks, explosion gases, shocks in water, and detonation in boosters. From the observations various deductions concerning detonator output can be made. For example, the velocities of shocks generated by detonators fired under water can be converted to peak pressures, which as functions of time or distance are relatable to the inherent output of the detonator. Similarly, the velocity of the air shock as a function of time is of value in comparing the relative levels of energy release from detonators, even though air shock plays only a minor role in initiation by detonators. Other techniques are used to measure the effective (usable) output in practical situations involving air gaps and heavy partial confinement. For very small gaps, the explosion gases play an important role in initiation. At some air-gap thicknesses, both loading by explosion gases and fragment impact are important in initiating detonation. If initiation is desired over a fairly wide air gap, fragment velocity is of particular importance.

It is desirable to include in the investigation experiments that show the effects on output and functioning characteristics of varying the electrical input to detonators. The performance of a detonator, primarily its functioning time, can be affected not only by the amount of input energy but also by the rate at which the energy is applied. Above a certain rate of application, the functioning time and the firing energy become essentially constant.

---

*References are on page 16.

It should be emphasized that this study is exploratory and we make no claim to finding an inexpensive, convenient, and precise way of measuring dynamic detonator output. From the results of the work, though, we are able to evaluate several techniques, make suggestions for improvements, and make recommendations for further study.

## II. EXPERIMENTAL

### A. Electrical Characteristics

#### 1. Electrical Measurements

Several test firings were made to determine the electrical response characteristics of the M84 detonator, Figure 1. Several known input firing pulses, ranging from 2 to 50 volts, were applied using an electronic pulsing unit with a variable voltage-capacitor discharge power supply. The unit was synchronized with our high-speed smear and framing cameras, so that simultaneous electronic and optical measurements of detonator response could be made. Figure 2 shows the silicon-controlled-rectifier-switch firing circuitry which was used to provide the input pulses. The capacitance value used was 2.15 microfarads.

Figures 3A and 3B, recorded in separate tests, are typical voltage-time and current-time oscillograms of the response of the M84 detonator to an input pulse of 5 volts. The potential across the detonator, Figure 3A, quickly reaches a 5-volt peak, gradually decays for ~23 microsec, then drops sharply, even appearing to become negative. The current-time record shows a quick rise to ~1.6 amps, then drops exponentially for ~23 microsec. At this point an abrupt increase in current occurs. The improved conductive path is probably due to the intense ionization produced by reaction of the lead azide in the detonator. Since the lead azide reacts rapidly, we consider that the interval from the beginning of the input pulse application to the beginning of the second current surge represents the time required for the initiation of the lead azide. Current flow peaks again at T = 24.5 microsec, then the detonator case ruptures and the conductive path is destroyed. The first 23 microseconds of the traces are typical of bridgewire heating. Initiation of the lead azide is indicated by the abrupt voltage and current changes that begin 23 microseconds after the voltage is applied. The lead styphnate spot ignited earlier but left no oscilloscope signature, since its products are only weakly ionized.

For input pulses of ~17 volts (current ~3 amp) and greater the oscillograms show a different response. In Figure 4A, e.g., the region of gradually decreasing voltage described above becomes a ramp after ~13 microsec. Up to this point the tungsten bridgewire, although heated rapidly during the initial part of the pulse, has not "burned out" or ruptured. Bridgewire "burnout" is indicated by the "open circuit" response of the current trace, Figure 4B (obtained in a separate test), and by the start of the "ramping" region in the voltage trace. The voltage ramp ends at T = ~20.5 microsec when the lead azide reacts sufficiently to produce ionization and hence restores

the conductive path and allows the capacitor discharge to continue. The current trace shows conductivity restored at T = ~17 microsec. Voltage and current traces recorded from the same test would be expected to show simultaneous occurrence of the ramp ending and the second current surge. Conductivity increases until the detonator case ruptures (T = 18.5 microsec) allowing conductive gases to escape. Note that case rupture occurred about 1.5 microsec after the lead azide initiation in both the 5-volt and the 17-volt tests.

2. Functioning and Initiation Times

The above interpretation of the electrical response of the M84 detonator allows a measure of detonator function times and internal initiation times versus the calibrated input pulses. In these measurements we consider the functioning time of a detonator as the interval between the beginning of the firing pulse and the rupture of the detonator case (see Figure 3). The initiation time is measured from the beginning of the input pulse to the time at which the initiation of the lead azide occurs.

Values of the initiation time, $\Delta T_1$ and functioning time $\Delta T_2$ that were determined from oscillograms of several input pulses are listed in Table 1. Also listed are values of $\Delta T_2^*$, the functioning time obtained from smear camera measurements of the initial detonator case expansion.* (Measurements of $\Delta T_2^*$ will be described in a later section of this report.) The data show that the initiation and functioning times become larger as the input pulse decreases from 50 volts to 2.6 volts. At 2.6 volts the detonator failed to fire.

B. Detonators Under Water (Aquarium Technique)

To quantitatively describe the output characteristics of a detonator, measurements may be made on the shock wave generated in a surrounding inert medium such as water. The measurements require an accurate knowledge of the equation-of-state of the inert material. Water, whose transparency permits continuous observation of the shock wave propagation by high-speed smear-camera photography, is most convenient for these measurements. Its Hugoniot equation-of-state is well known.

Figure 5 shows the aquarium arrangement used for observations of the motion of the underwater shock wave from an M84 detonator. The shock wave motion is delineated by shadowgraph photography using a field lens and the light from an exploding tungsten wire. The 0.025-mm diameter tungsten wire is confined in a 100-mm length of glass capillary tubing. Energy to the wire is supplied by the sudden discharge of a 4-μf capacitor charged to 4 kv. In these measurements an auxiliary lensing arrangement was used to obtain an object-to-image ratio of 1:2, covering the first 13-17 mm of shock propagation in the water.

---

* Accuracy of the $\Delta T_2^*$ values is in doubt. After the tests were run, some intermittent malfunction of the electronic delay equipment was discovered, which possibly could have been present during the test series.

TABLE 1

INTERNAL INITIATION AND FUNCTIONING TIMES OF THE M84 DETONATOR

| Input Pulse (volts) | $\Delta T_1$ (microsec) | $\Delta T_2$ (microsec) | $\Delta T_2^*$ (microsec) |
|---|---|---|---|
| 50 | 13.6 | - | 14 |
| 38 | 17.0 | - | 18 |
| 17 | 20.5 | - | - |
| 17 | 20.5 | - | - |
| 17 | 16.0 | 18.0 | - |
| 12 | 21.0 | - | 19 |
| 12 | 22 5 | 24.0 | - |
| 5 | 23.5 | 25.5 | - |
| 5 | 23.7 | - | - |
| 5 | 31.3 | - | 31 |
| 4 | 32.0 | - | - |
| 2.6 | Failure | - | - |

1. Axial Shock Wave Measurements

Smear-camera measurements of the transmitted shock wave velocity in water along the extended axis of the detonator allow one to ascertain, using the water shock Hugoniot, the shock pressure transmitted by the detonator casing. From the knowledge of this pressure an estimate can be made of the pressure in the detonation wave initiated in the explosive column. This estimate requires that the detonator tip be very thin. Also, the effect of the peak pressure (von Neumann spike) in the non-reactive shock ahead of the detonation wave must be ignored. On the other hand, the experimentally measured shock state in the water can be compared with the calculated shock state which is obtained from knowledge of the detonation pressure of the explosive and the shock Hugoniots of the detonator casing material and water. This procedure was chosen and the experimental measurements and the calculations of the initial shock state in the water are described below.

Figure 6 shows a smear-camera shadowgraph of the motion of the shock wave imparted to water by the base end of an M84 detonator. Shock wave velocities were obtained by differentiation of the distance-time data derived from micro-comparator readings of the trace. Figure 7 gives details of the shock wave velocity decay for positions in the water out to 17 mm from the detonator tip. (Sonic velocity[4] in distilled water is 1481.63 m/sec at 20°C.) The extrapolated initial shock velocity imparted to the water at the detonator tip was 3820 m/sec. This velocity corresponds to a peak pressure in the water of 46.7 kbar (see reference 5).

The calculated initial shock state is obtained using the impedance matching conditions. The method requires knowing the reflected shock adiabat of PETN explosion products. Assuming a gamma law expansion of the explosion products from the detonation state, the reflected pressure, $P_2$, and the particle velocity, $u_2$, are computed from

$$u_2 - u_1 = \frac{2C_1}{\gamma-1}\left[1 - \left(\frac{P_2}{P_1}\right)^{(\gamma-1)/2\gamma}\right] . \qquad (1)$$

(This relation is equation 18 of reference 6.) For the calculation, the density of PETN in the M84 detonator was assumed as 1.56 g/cm³. Then in equation (1) the detonation pressure, $P_1$, is 240 kbars[6], the particle velocity at the front, $u_1$, is 1960 m/sec, the sound velocity, $C_1$, is 5830 m/sec and the isentropic exponent, $\gamma$, is 2.97. The impedance-matching solution for the initial shock state in the water is shown in Figure 8. Here the reflected PETN adiabat intersects the steel shock Hugoniot (references 7 and 8) to indicate a pressure of 390 kbars transmitted into the stainless steel detonator cup. The Hugoniot curve for steel reflected through this point intersects the water shock Hugoniot to give a predicted initial shock pressure of approximately 70 kbars in the water. This value is

~40% greater than the experimental result. The difference is expected, principally, because the assumed detonation state parameters for the PETN in the detonator are for an infinite diameter charge, and the diameter effect was not considered.

2. Lateral Shock Waves

With the smear camera slit image aligned at 90 degrees with respect to the detonator casing, rather than parallel (axially) as in the end-shock measurements, one obtains a record of the laterally generated shock waves on each side of the detonator. Figure 9 is a record obtained using this arrangement. The camera slit image was aligned 2.3 mm from the end of the detonator, and a camera writing speed of ~4 mm/microsec was used. The record shows that the shock trace in water is more clearly delineated than in the record of the shock wave from a detonator fired in air.* Note the large difference in the initial decay of the shock wave traces from each side of the detonator casing. The initial velocities measured from the early and later traces are 2.20 mm/μsec and 3.30 mm/μsec respectively. There is a surprising time difference, 0.57 μsec, between the initial points of these two traces. The M84 bridgewire is off-center (see Figure 1), but the observed asymmetry is about twice as great as design geometry alone would imply for a position 2.3 mm from the end of the detonator.

3. Detonator Product-Gas Bubble in Water

Framing camera shadowgraphs made with the focal-plane shutter framing camera[9] were used to obtain photographic details of the underwater initiation of the M84 detonator. A sequence of frames with 1.1 microsec between frames is shown in Figure 10. Asymmetry in the shock wave and product gas expansion is again present, but somewhat exaggerated here because time increases from top to bottom in each of the frames shown (see reference 9). In the second frame the shock wave is a well-defined expanding spherical wave, ~20 mm in diameter. An early shock can be seen at the detonator plug end. Its presence is not readily explained. At 3.3 microsec, frame 4, the fragments both radially from the casing sides and axially from the detonator tip are visible in the region between the product gas bubble and the expanding water shock wave. This region displays very fine shock detail, e.g., schlieren effects which probably occur from interactions between the gas bubble and the case fragments. The case fragments in the aquarium firings were generally recovered; the M84 detonator cup bottom was recovered intact.

C. Detonators Initiated in Air

1. Framing Camera Observations

Figure 11 is a sequence of framing camera shadowgrams of the shock expansion events resulting from the initiation of the M84 detonator in air. The time interval between frames is 2.7 microsec, and the distance between the two magnification tapes within each frame is 12.7 cm. The frames show the explosion products expansion, the propagation of the air shock resulting from the initiation, and the motion of the fragments from the detonator case.

*See page 27 of this report.

In contrast to the underwater shots where the end-pieces of the detonator case were recovered intact, the ends of the stainless steel case are broken up into a number of pieces when the M84 detonator is fired in air. Careful inspection of Figure 11A shows that the end piece broke into seven fragments. The mean velocities of the several fragments in four detonator firings are listed in Table 2. Also given is the range of velocity between the fastest and slowest fragments. The velocity measurements were made over 120 mm. Fragment patterns were obtained by locating cardboard targets about 180 mm away from the detonators. The patterns of holes in the cardboard show the fragments struck within circles of 18-mm to 26-mm diameter.

TABLE 2

M84 DETONATOR CASE FRAGMENT VELOCITIES IN AIR

| Shot Number | Mean Velocity of Several Fragments (mm/microsec) | Velocity Range (mm/microsec) |
|---|---|---|
| 1 | 2.00 | 1.87 - 2.15 |
| 2 | 1.99 | 1.80 - 2 |
| 3 | 2.02 | 1.85 - 2.20 |
| 4 | 2.05 | 1.91 - 2.23 |

2. Smear Camera Observations

a. Axial Case Expansion

In several tests smear camera measurements of detonator output were made simultaneously with determinations of the M84 detonator's electrical characteristics. Figure 12A is a view of the smear camera alignment of the detonator assembly for these tests. Figure 12B is a typical smear camera shadowgraph trace of these firings. The following events occur in Figure 12B:

(1) A timing pip trace made by synchronizing the explosion of a tungsten bridgewire with the beginning of the input pulse is shown above.

(2) The detonator case expansion begins at this time.

(3) The product gases expand from the case.

(4) This time denotes the impact of the detonator case fragments with the target plate noted in Figure 12A.

Table 3 summarizes a series of M84 detonator firings in air.

The input pulses were between 5 volts and 50 volts from a 2.15 microfarad capacitor. Table 3 lists: (a) the time between the beginning of the pulse input and the start of detonator case expansion (this time is the detonator functioning time, $\Delta T_2^*$, described previously); (b) the case velocity; (c) the gas-cloud velocity; and (d) fragment energy. The estimates of fragment energy are based on the M84 detonator cup bottom velocity and weight.

TABLE 3

M84 DETONATOR SHOCK CHARACTERISTICS IN AIR

| Detonator Input (volts) | Functioning Time (μsec) (a) | Case Velocity (mm/μsec) | Gas Velocity (mm/μsec) | Fragment Energy (cal/cm$^2$) (b) |
|---|---|---|---|---|
| 50 | 14 | 1.68 | 2.55 | 46.2 |
| 38 | 18 | 1.62 | 2.64 | 44.6 |
| 38 | 19 | 1.49 | 2.63 | 41.0 |
| 12 | 19 | 1.43 | 2.72 | 39.4 |
| 5 | 31 | 1.57 | 2.56 | 43.2 |

(a) Time from beginning of input pulse to initial motion of detonator case.
(b) Weight of cup bottom = .021 gram. Cup bottom area = .153 cm$^2$.

There is an indication in these data that a low case velocity allows a higher gas velocity which may make the overall detonator performance appear uniform, particularly if both the detonator case fragments and gaseous explosion products contribute to the transfer of detonation. For example, a slower expanding case may permit a longer time for gas confinement, higher pressure build up, and therefore, a higher gas velocity after the case ruptures.

b. Lateral Case Expansion

Figure 13 is a smear camera record showing lateral expansion of the detonator casing and product gas break out. Figure 14 shows distance-time profiles taken from the lower trace of Figure 13. Typically, the initial lateral case velocities from the top and bottom traces showed asymmetrical initiation. For example, initially, the top trace of Figure 13 gave a velocity of 0.91 mm/microsec, the bottom trace, 1 41 mm/microsec. Maximum velocities of 2.11 mm/microsec and 2.05 mm/microsec respectively, occurred just before product-gas breakout.

## D. Build up to Detonation in Booster Explosives

When a high explosive is initiated by a shock, detonation most often does not start immediately at the HE input surface. Instead, a run distance to detonation may occur, typically one or two millimeters long for a strong shock initiating a fairly sensitive explosive[10,11]. The run distance (or delay time) increases as the initiating shock strength decreases, with the most marked increase occurring when the critical shock strength for detonation is barely exceeded. By measuring the run distance to detonation it is possible to detect small differences in the effective strength of initiating shocks, assuming adequate uniformity throughout the rest of the explosive system. The sensitivity of such a detection method is best when the shock strength is just slightly more than enough to produce detonation.

### 1. Experimental Arrangements

Because explosive leads are confined and usually quite small, special techniques are needed to observe the arrival of detonation along the cylindrical surface of the booster. A set-up for use in recording the detonation trace in a simple detonator/booster system is shown in Figure 15A. The detonator, an Atlas microdetonator, shown in detail in Figure 16, is confined in an aluminum holder. The booster is a 4.3-mm diameter by 6.6-mm long tetryl pellet (density = 1.54 g/cm$^3$) laterally confined in a steel holder. Both the top and bottom surfaces of the booster are bare. The arrangement is the same as used in making dent tests. Observation is by smear camera.

In order to directly observe the bare cylindrical surface of the tetryl booster, a 0.2-mm wide slot is cut completely through the wall on one side of the steel holder and parallel to the axis of the system. (The effect on confinement caused by the presence of the slot is considered to be negligible.) About 1.5 mm of the 6.6-mm long slot at the top of the booster holder is filled in with epoxy cement containing iron powder. This prevents detonation light, transmitted through the slot, from being obscured by air shock and explosion gases. Also, considerable care is required in cementing the top periphery of the booster holder to the inside surface of the detonator holder. A good seal here is necessary to prevent air shock and explosion gases from getting through prematurely. To permit observation over the entire unplugged (5-mm) portion of the slot, it is necessary to cut a short slot through the wall at the base of the aluminum detonator holder. Otherwise, the useful slot length is only 3.8mm.

In making a shot, the slit of the smear camera is aligned with the bridgewire used to indicate when the detonator is energized; the slot in the booster holder; and a 1-mm diameter hole drilled through the wall of the detonator holder to indicate when the detonator fires (Figure 15A). The camera slit is used only for alignment and is removed when the shot is fired. The detonators in some of the

shots are energized by fast-rising pulses of high energy; 4μf at 2 kv. In the remaining shots a relatively low energy is used; 2.2 μf at 45 v. The exploding bridgewire is connected in series with the detonator in the high-energy shots. In the low-energy shots the bridgewire is energized simultaneously with the detonator by a separate high-energy pulsing unit. Incidentally, a threaded hole, originally made in the detonator holder for a set screw, is plugged with metallized epoxy cement. Even with the screw in place, there may be enough air space left around the detonator to affect the lateral confinement appreciably.

2. Run-Distance Results

In studying variations in detonator output by the run-distance-to-detonation technique, it is necessary to establish conditions which are close to critical for detonation in the booster. The detonation trace shown in Figure 15B was obtained under nearly critical shock conditions in the booster. Detonation is shown breaking out first on the cylindrical surface of the booster at a distance, S, from the top of the booster. The distance, S, here is assumed to be equal to the run to detonation down the axis of the booster. Also shown is the time taken for the detonator to fire, $\tau_1$, and the time for detonation to reach the bottom of the booster, $\tau_2$, after the detonator fires.

The run-to-detonation results of eight shots with the Atlas microdetonator are given in Table 4. Also included are the times, $\tau_1$ and $\tau_2$. In Shots 1, 2, 3, and 7, where the air gaps were 6.64, 6.65, 3.99, and 3.61 mm, respectively, the booster failed to detonate. (On the basis of results obtained by other workers, it appeared that the Atlas microdetonator might initiate the tetryl booster over air gaps of 3.82 mm or more.) Detonation occurred in Shots 4, 5, 6, and 8, where air gaps were 0.84, 1.27, 2.54, and 3.66 mm, respectively. Shots 4 and 5 were fired to establish the shape of the detonation trace for a relatively high level of energy transfer from the detonator. As expected, in the latter two shots the run distance to detonation, S, was too short to be observed, since the first break-out of detonation occurred in the blind (plugged) section of the slot cut in the booster holder. Accordingly, the run distances for these two shots are listed as less than 1.5 mm in the table.

In Shot 7, note that the booster failed to detonate using a 3.61-mm air gap, but the booster in Shot 8 detonated using a slightly larger gap. However, the tetryl booster in Shot 8 was resting on a 6-mm thick plate of aluminum. In all of the other shots the booster was unconfined at the bottom. The presence of the aluminum plate may have had some effect on the initiation, but this does not seem likely from the appearance of the detonation trace. Superposed sketches of detonation traces from Shots 5, 6, and 8 are shown in Figure 17. In Shot 6, with a 2.54-mm gap, the upper portion of the detonation trace shows more curvature than in Shots 4 and 5. It is apparent from the shape that the run distance to detonation is longer in Shot 6 than it is in Shots 4 and 5. It is estimated to be close to the length of the blind portion of the slot in the booster holder,

i.e., S = 1.5 mm. In Shot 8, with a 3.66-mm air gap, the curvature is even more pronounced. In all four shots showing detonation in the booster the detonation velocity reached a phase velocity of nearly 800 m/sec. (The true velocity should be close to 7000 m/sec.)

From the results, it appears that the critical air gap should be close to 3.65 mm. However, a reasonable number of shots should be made to establish the reproducibility at a fixed air gap distance. Undoubtedly, a number of improvements could be made in the technique. The slot system in the booster holder should be redesigned to reduce the difficulty in making alignments and to improve the quality of the detonation trace. If enough detonation light is made available, the slit system of the camera should be used in order to obtain more precise timing markers. The microdetonator may have been an unfortunate choice in the exploratory series, since the end of the detonator is concave. This causes a jet to form which could make the initiation more complicated than if a flat-ended detonator, such as the M84, were used.

The detonator firing times, $\tau_1$, in Table 4, were uniform for high-energy input but varied from 2.4 μsec to 32.4 μsec when a 45-volt firing pulse vas used. Such variation may be typical for this detonator under "low-energy" firing conditions. However, since a separate pulsing unit was used to explode the reference bridge-wire in the "low-energy" firings, further tests are needed to firmly establish this detonator's inherent functioning time variation.

TABLE 4

RUN-DISTANCE RESULTS FOR TETRYL INITIATED BY THE ATLAS MICRODETONATOR

| Shot Number | Air Gap (mm) | Reaction In Booster | $\tau_1$ (μsec) | $\tau_2$ (μsec) | S (mm) |
|---|---|---|---|---|---|
| 4 | 0.84 | Detonated | 6.8 | 1.3 | <1.5 |
| 5 | 1.27 | Detonated | 2.4 | 1.0 | <1.5 |
| 6 | 2.54 | Detonated | 12.4 | 1.3 | ~1.5 |
| 7 | 3.61 | Failed | 11.7 | - | - |
| 8 | 3.66 | Detonated* | 32.4 | 2.1 | 2.5 |
| 3 | 3.99 | Failed | 1.7 | - | - |
| 1 | 6.64 | Failed | - | - | - |
| 2 | 6.65 | Failed | 1.4 | - | - |

*Tetryl booster rested on a 6-mm thick Al plate.

Note: Shots 1, 2, and 3 were made with high-energy input to detonator.

## III. DISCUSSION AND RECOMMENDATIONS

In Table 5, the detonator evaluation experiments are summarized in terms of their primary advantages, disadvantages, and estimated cost. The priority recommendations of Table 5 are based on likelihood of substantial benefit at reasonable cost. It is difficult to devise a means of accurately measuring the dynamic output of a detonator. Any errors in making a measurement must be reasonably small compared to actual variations in detonator output. The chief difficulties arise from the small size of detonators and the extremely high rate of chemical reaction of the explosives involved. In addition, the available output of energy for a given application will depend on how the detonator is oriented and confined. This is true even if the total inherent energy release is the same from detonator to detonator. Heavy confinement of part of the detonator will cause energy to concentrate in regions of lesser confinement. For example, if the detonator is heavily and confined radially, but not at the end, more of the total energy is expended axially from the end of the detonator. It follows, then, that variations in the immediate environment of the detonator, such as in clearances and alignment, can cause variations in effective output in a particular application. Also, the very process of making output measurements can contribute to observed variations in output.

### A. Electrical Characteristics

Precise knowledge of the functioning time of a detonator helps to determine the applicability of a device for a specific function. Here we have defined the functioning time of a detonator as the time elapsing between the beginning of the input pulse and the initial (free-surface) motion of the detonator case. Functioning times of the M84 detonator (and initiation times of its lead azide) were shown to be related to the magnitude of the calibrated electrical input pulse for the low energy inputs. The times were determined from an interpretation of the oscillograph records of the electrical behavior of the detonator and from smear camera measurements of detonator case expansion.

Other methods recommended for determining detonator functioning times include use of air gap ionization, sound output, light output using photomultiplier circuitry, and triggering of pin probe switches by case motion. Measurements using pressure transducers also are recommended.

### B. Underwater Measurements

The underwater shock wave measurements gave substantial information directly relatable to accurate pressure calibration of the detonator output. High speed photography revealed a very sharply defined shock wave propagating through the water. Detonator product gas expansion and flight of case fragments were also recorded, and the case fragments were readily recovered. The characteristics of

TABLE 5

COMPARISON OF DETONATOR EVALUATION EXPERIMENTS

| Experiment | Primary Advantage | Primary Disadvantage | Estimated Cost | Priority For Further Work |
|---|---|---|---|---|
| Booster Response Measurements | Identifies marginal initiation conditions | Complicated to perform | High | 1 |
| Underwater Shock Pressure Measurements A. Pressures obtained by photography | Measures shock pressures transmitted into a well calibrated medium | Complicated to perform | Moderate | 2 |
| B. Pressures obtained by pressure transducers | Measures shock pressures transmitted into a well calibrated medium | Requires gage calibration | Relatively Low | 1 |
| Case Fragment Velocities A. Close-in | Precise measurement of case expansion rate at early time | Fragments are only one of several contributors to transfer of detonation | Moderate | 2 |
| B. Distant | Measures final velocity of the fragments | Position of measurement is remote from where detonation transfer contributions are made | High | 3 |
| Explosion Gas Velocities | Measures gas expansion velocity at early time | Explosion gases are only one of several contributors to transfer of detonation | Moderate | 2 |

the shock wave formed in water by detonator initiation are different than for air, due to water's thousand-fold greater density. This allows high-speed photography to reveal details of detonator response not readily distinguishable during initiation in air.

In these output measurements the velocity of the underwater shock wave was used to obtain an indirect measurement of pressure in the water. However, the use of pressure transducers is readily adaptable and is recommended here. Particularly adaptable are small tourmaline (piezoelectric) gages[12] and carbon gages[13] which can be calibrated dynamically. A carbon resistor (~560 ohms), costing a few cents has been used as a very cheap gage suitable for output measurements in the transmitted pressure range.

There is good justification for recommending adaptation of the high-speed photographic measurements of lateral shock wave propagation and case expansion to determine output, especially where there is a need to develop and fully evaluate explosive components. These measurements are particularly significant when compared to similar measurements of the propagation occurring axially beyond the end of the detonator. For example, maximum lateral shock wave pressures from the M84 detonator were ~60% lower than the axial values. Similar pressure differences are expected in other detonators. Also, the asymmetric initiation which occurs in the M84 produced distinct differences in lateral shock break-out times and in initial pressures on opposite sides of the detonator. A complete knowledge of the pressure and time variations around the detonator can aid the design of side initiators, give insight into reliability of initiation, and reveal variations in loading of the explosive elements of the detonator.

C. Case and Gas Expansion in Air

The detonator fragment and gas-cloud velocity measurements are recommended as reliable indicators of the variance in detonator output. Concurrent with the course of this study, additional proof was obtained showing the value of these measurements in distinguishing differences in performances of explosive systems. Detonators,* each presumably loaded identically, were prepared by two different manufacturers. One manufacturer's detonators gave a large percentage of charge initiation failures. Investigation of detonator performance using the plate-dent test failed to distinguish a difference between the two lots of detonators. However, smear camera measurements of gas-cloud velocities revealed an ~20% velocity difference between detonators. The detonators with the lower velocities were the ones that were unreliable.

D. Detonation Build-up in Booster Explosives

The run-to-detonation data show that progress can be made in devising a dynamic method for relating the variance in detonator

*The base charge in this detonator is 100 mg of hexanitrostilbene (HNS). The casing is stainless steel.

output with the performance of integral parts of an explosive system. However, despite the promising records which show the feasibility of the run-to-detonation technique, the technique does have some shortcomings. For one thing, the critical condition for failure is approached fairly abruptly. This makes the useful range for detecting variations in effective detonator output very narrow. When the detonation trace is used as the only indicator, it is not possible, of course, to tell how close conditions were to causing detonation when failure occurred.

It is recommended that tests employing a "flying foil" technique[14,16] be used to increase the useful information. One might try placing a thin (but not too thin) layer of tough inert material in flat contact with the end of the booster. If any appreciable chemical reaction occurs in the booster, the layer of inert material will fly off with a higher velocity than if no chemical reaction occurs. Back-lighting would be used to shadowgraph the motion. The system could be calibrated by obtaining the free-surface velocity of the inert layer as a function of air gap thickness. By this method it may be possible to tell in a comparatively few shots how close conditions are to producing detonation in boosters.

## IV. REFERENCES

1. "Measuring Output, Safety and Reliability of Explosive Components," Robert K. Warner, HDL-TM-71-34, Nov 1971.

2. "A Review of Explosive Output Testing," V. J. Menichelli, Proceeding of Electric Initiator Symposium, 1-2 Oct 1963; AD 440 764.

3. "Factors Affecting the Output of Electric Detonators," R. Stresau et al, Electric Detonators: Proceedings of the Symposium 14-15 Sep 1954; AD 066 001.

4. W. D. Wilson, J. Acoust. Soc. Amer., 31, 1067 (1959).

5. M. H. Rice and J. M. Walsh, J. Chem. Phys., 26, 824 (1957).

6. N. L. Coleburn, NOLTR 64-58 (1964).

7. F. S. Minshall, J. Appl Phys., 26, 463 (1955).

8. S. Katz, D. G. Doran, and D. R. Curran, J. Appl Phys., 30, 568 (1959).

9. S. J. Jacobs, J. D. McLanahan, and E. C. Whitman, J. SMPTE 72, 927 (1962).

10. S. J. Jacobs, T. P. Liddiard, and B. E. Drimmer, "The Shock-to-Detonation Transition in Solid Explosives," 9th Symposium (International) on Combustion, 517-26, Academic Press, N.Y.C. (1963).

11. A. W. Campbell, W. C. Davis, and J. R. Travis, Phys. Fluids, 4, 498, (1961).

12. J. R. Hearst, G. B. Irani, and L. B. Geesaman, J. Appl. Phys. 36, 3440 (1965).

13. R. W. Watson, Rev. Sci. Inst. 38, 978 (1967).

14. E. F. Gittings, 4th Symposium on Detonation, Naval Ordnance Laboratory, White Oak, 12-15 Oct 1965, ACR 126.

15. T. P. Liddiard, Jr., 4th Symposium on Detonation, Naval Ordnance Laboratory, White Oak, 12-15 Oct 1965, ACR 126.

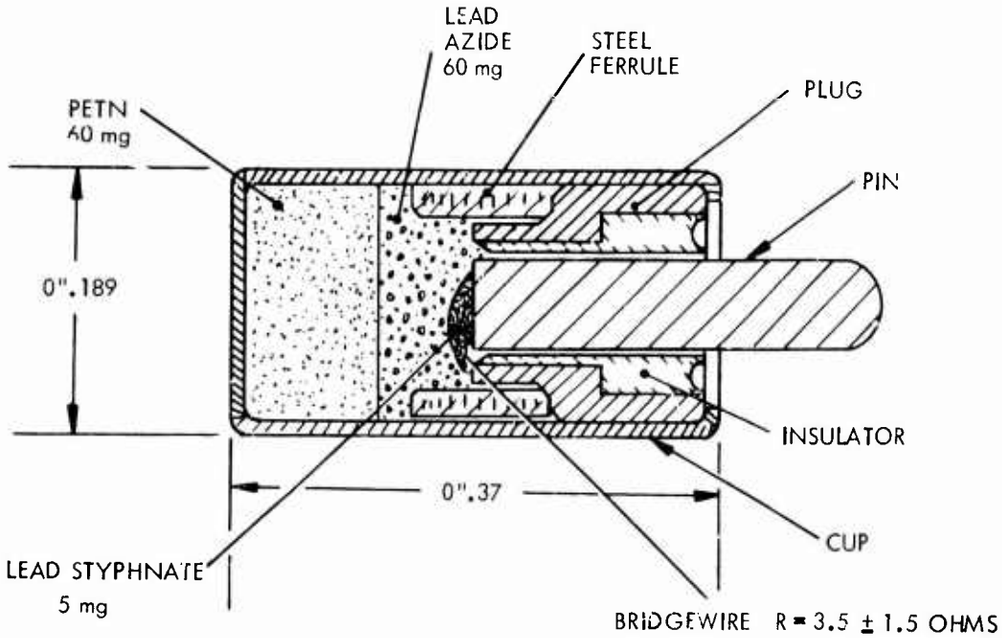


FIG. 1 M84 DETONATOR

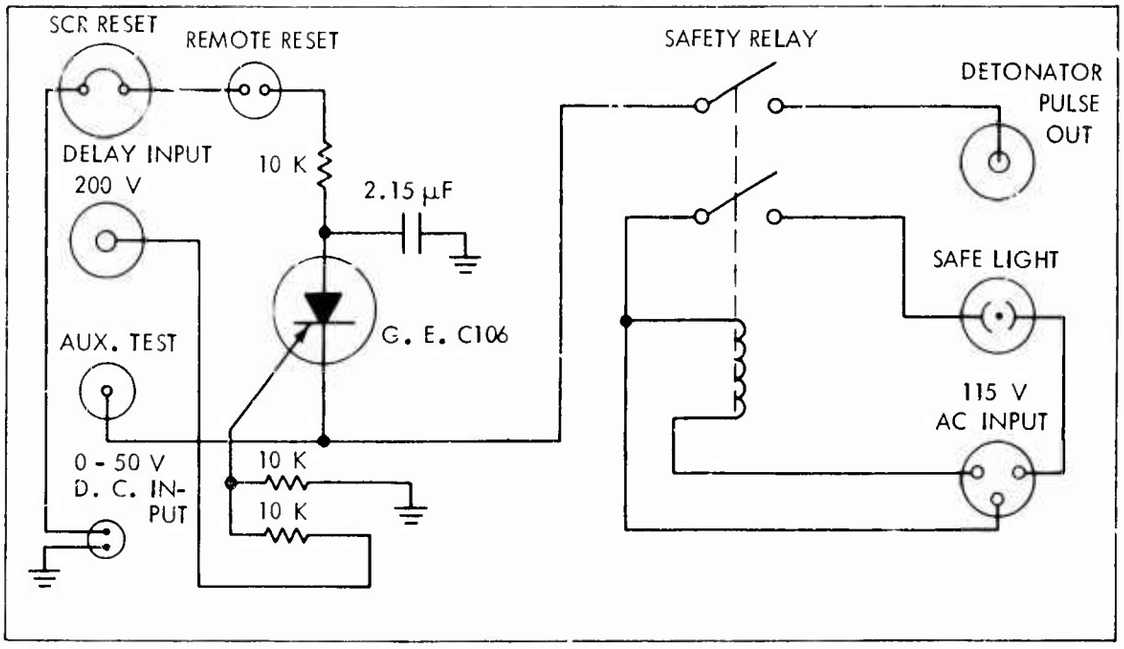


FIG. 2 FIRING CIRCUIT

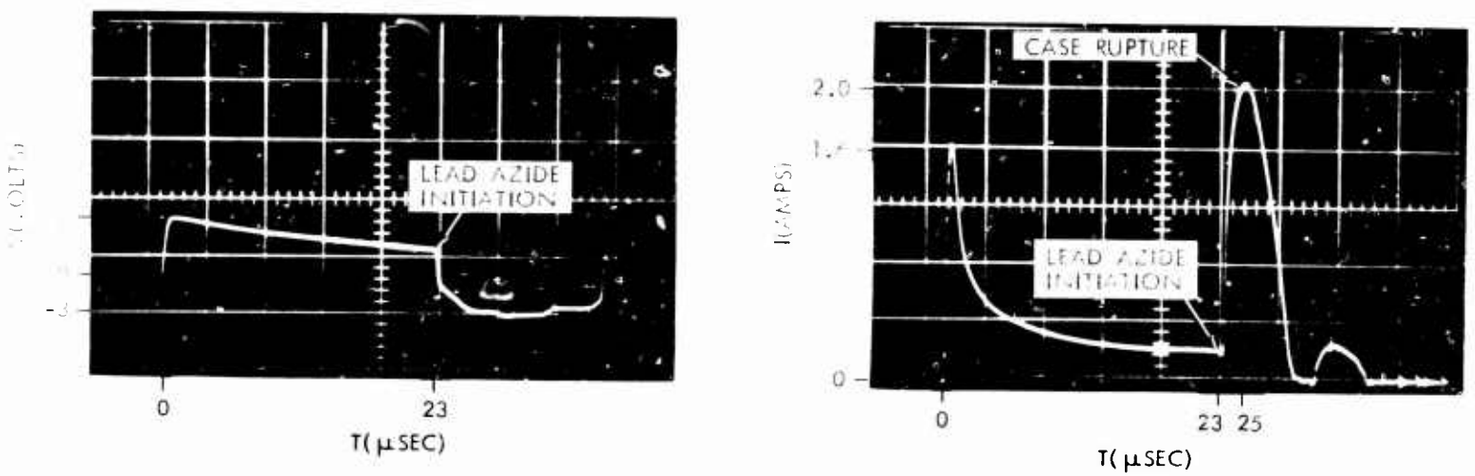


A. B.

FIG. 3 OSCILLOGRAMS OF M84 DETONATOR ELECTRICAL RESPONSE TO A 5-VOLT INPUT PULSE

A. VOLTAGE-TIME (5 V/DIV - 5 μSEC/DIV), TEST 8

B. CURRENT-TIME (0.4 A/DIV -5 μSEC/DIV), TEST 13

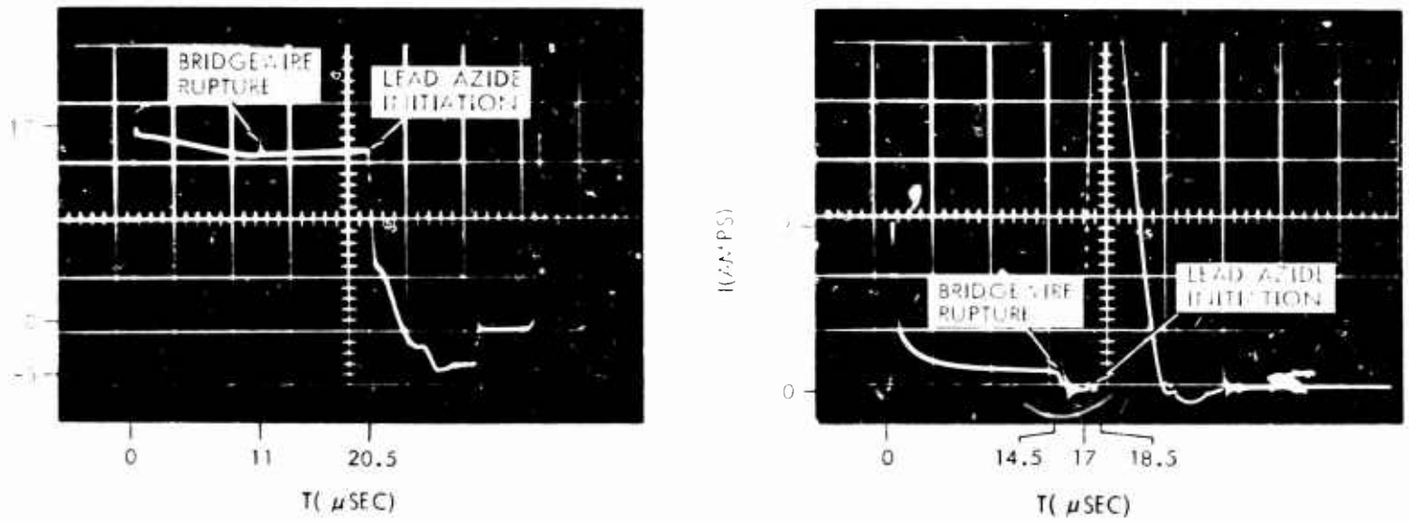


FIG. 4 OSCILLOGRAMS OF M84 DETONATOR ELECTRICAL RESPONSE TO A 17-VOLT INPUT PULSE

A. VOLTAGE-TIME (5 V/DIV - 5 μSEC/DIV), TEST 11

B. CURRENT-TIME (1 A/DIV - 5 μSEC/DIV), TEST 12

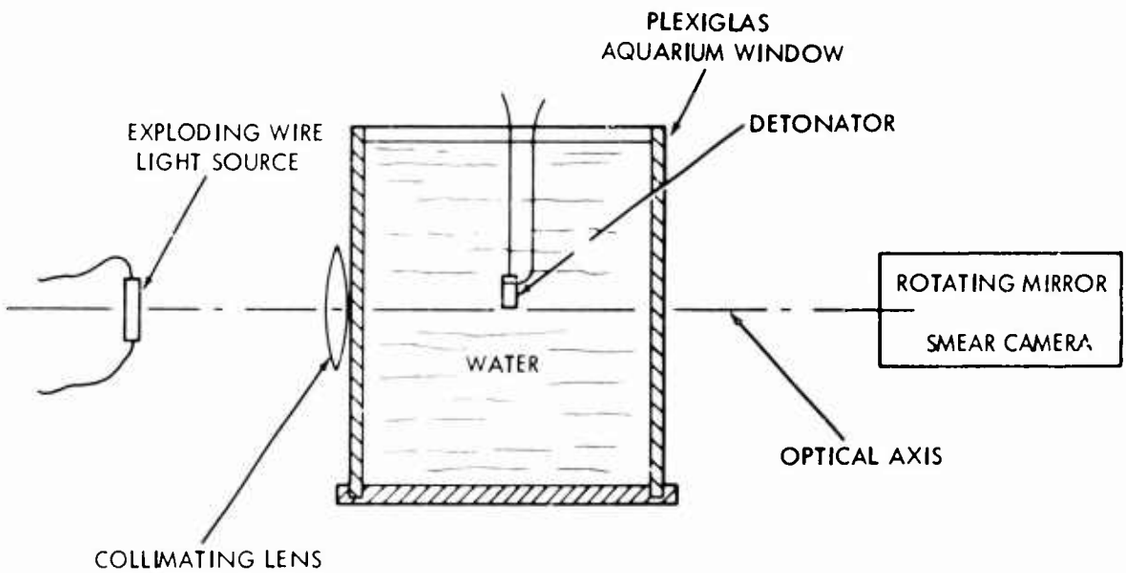


FIG. 5 THE AQUARIUM ARRANGEMENT FOR MEASURING DETONATOR OUTPUT IN WATER

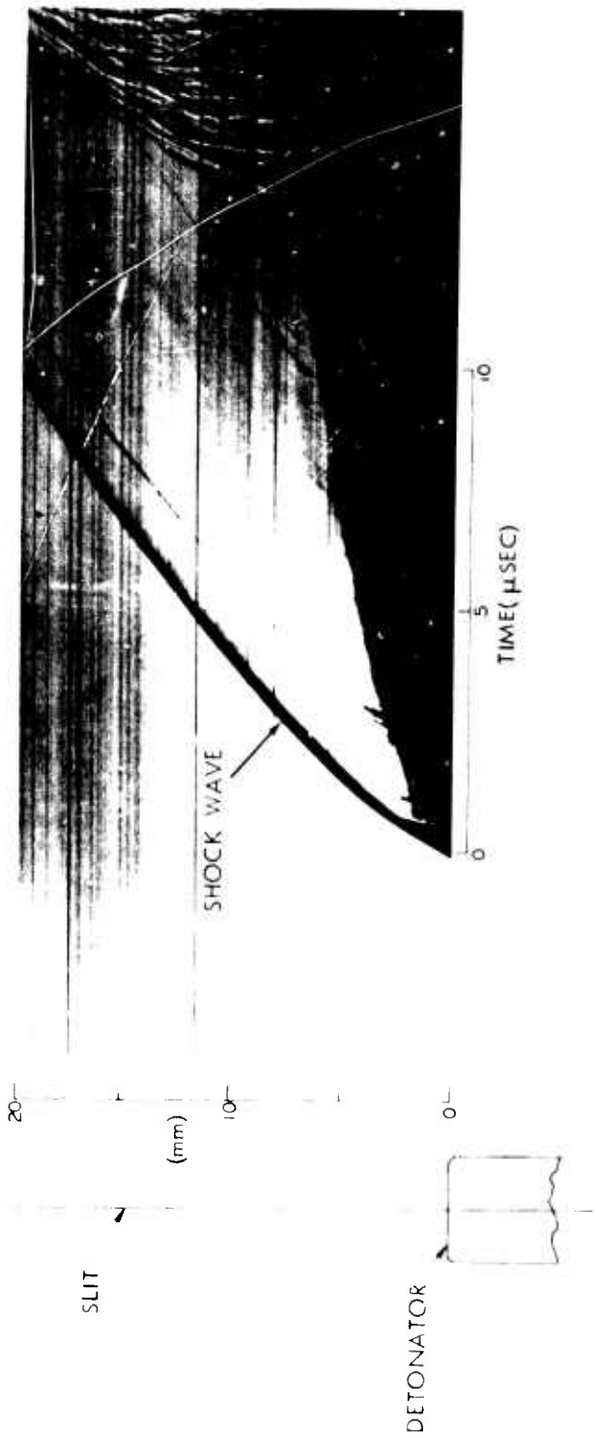


FIG. 6 SMEAR CAMERA SHADOWGRAPH OF AXIAL SHOCK WAVE MOTION PRODUCED BY THE M84 FIRED UNDERWATER

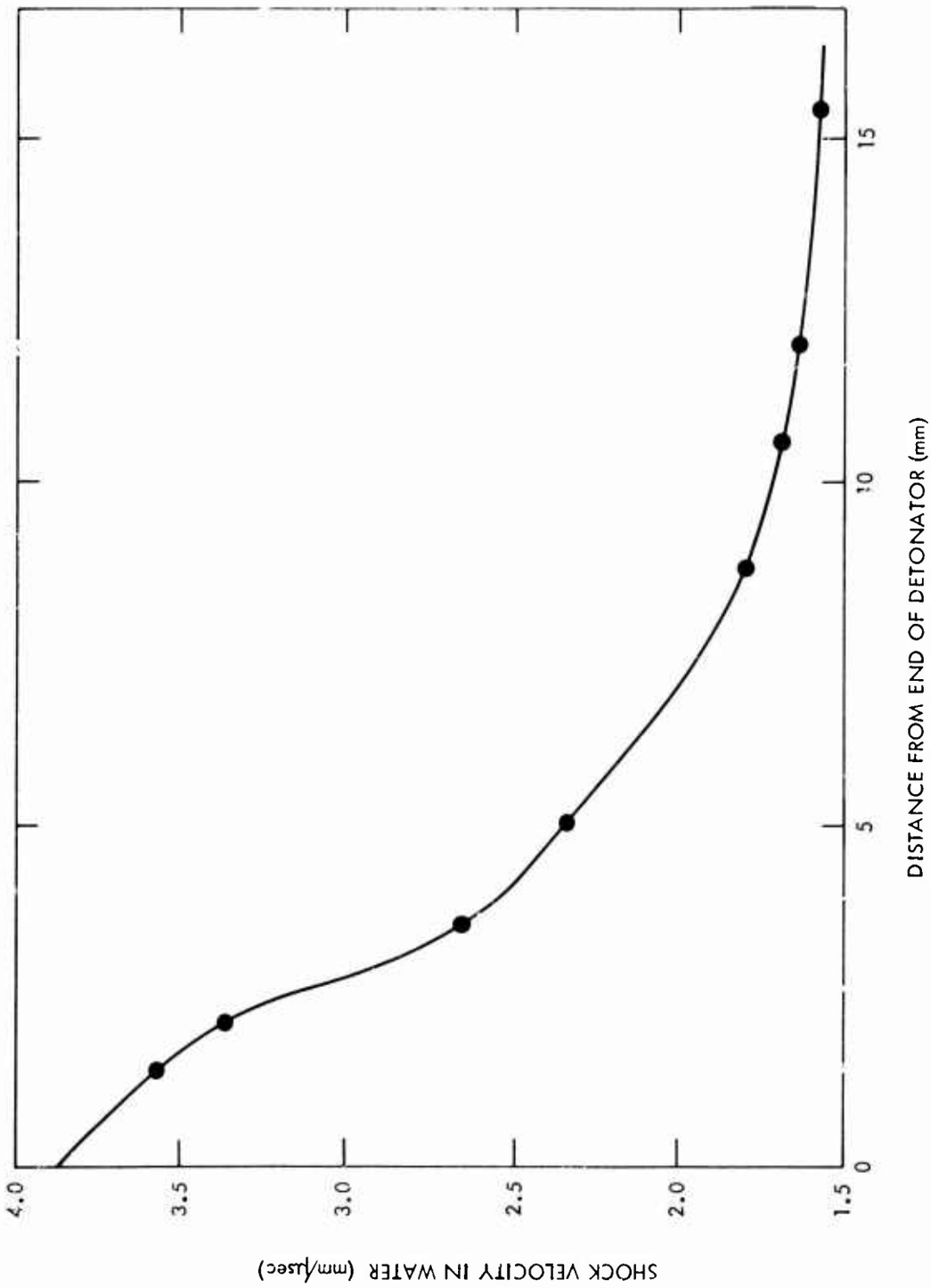


FIG. 7 UNDERWATER SHOCK WAVE VELOCITY DECAY

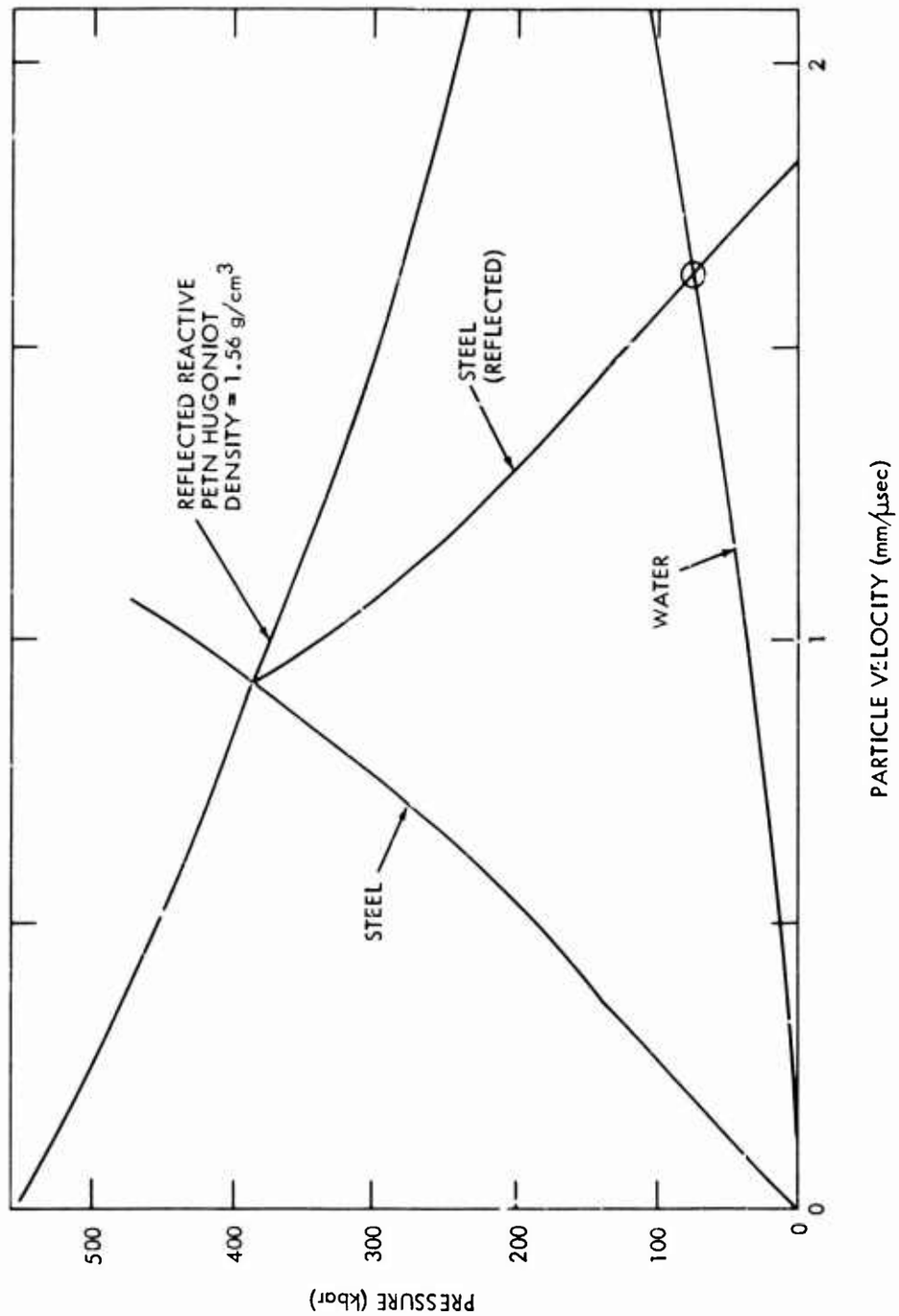


FIG. 8 IMPEDANCE MATCH SOLUTION FOR PEAK PRESSURES TRANSMITTED INTO WATER BY THE M84 DETONATOR

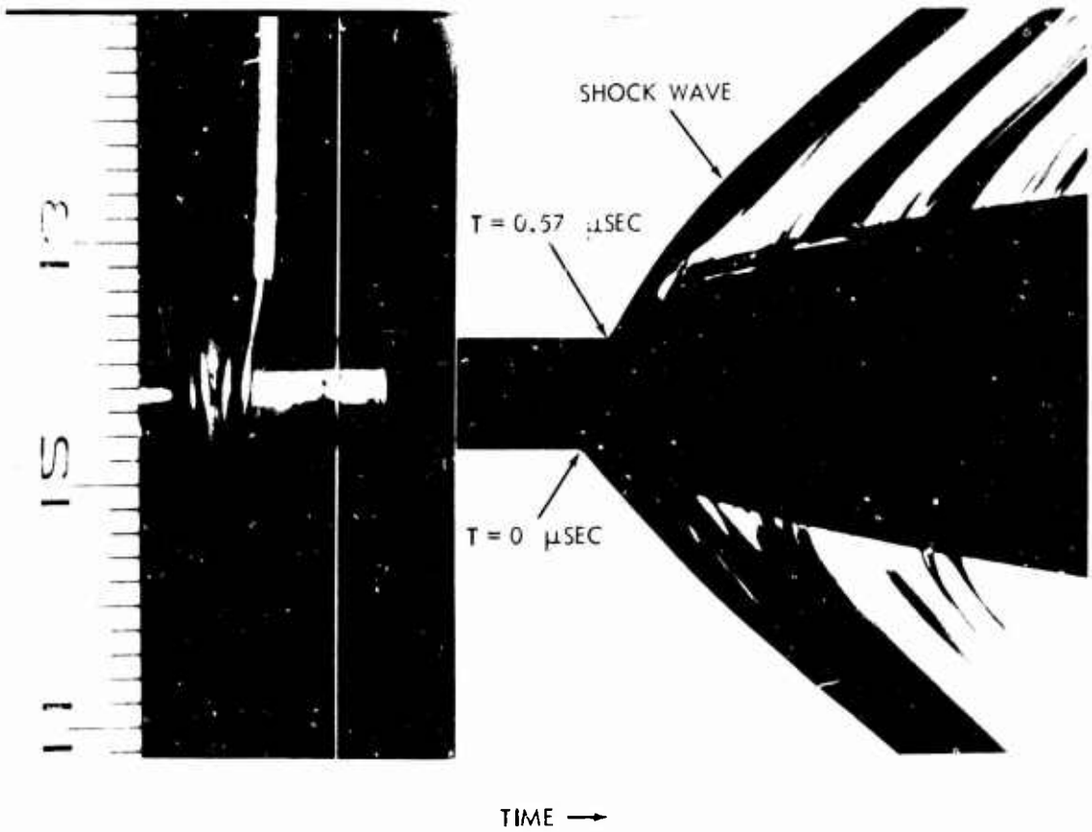


FIG. 9 SMEAR CAMERA RECORD OF LATERAL SHOCK WAVE EXPANSION FROM THE M84 DETONATOR FIRED UNDERWATER

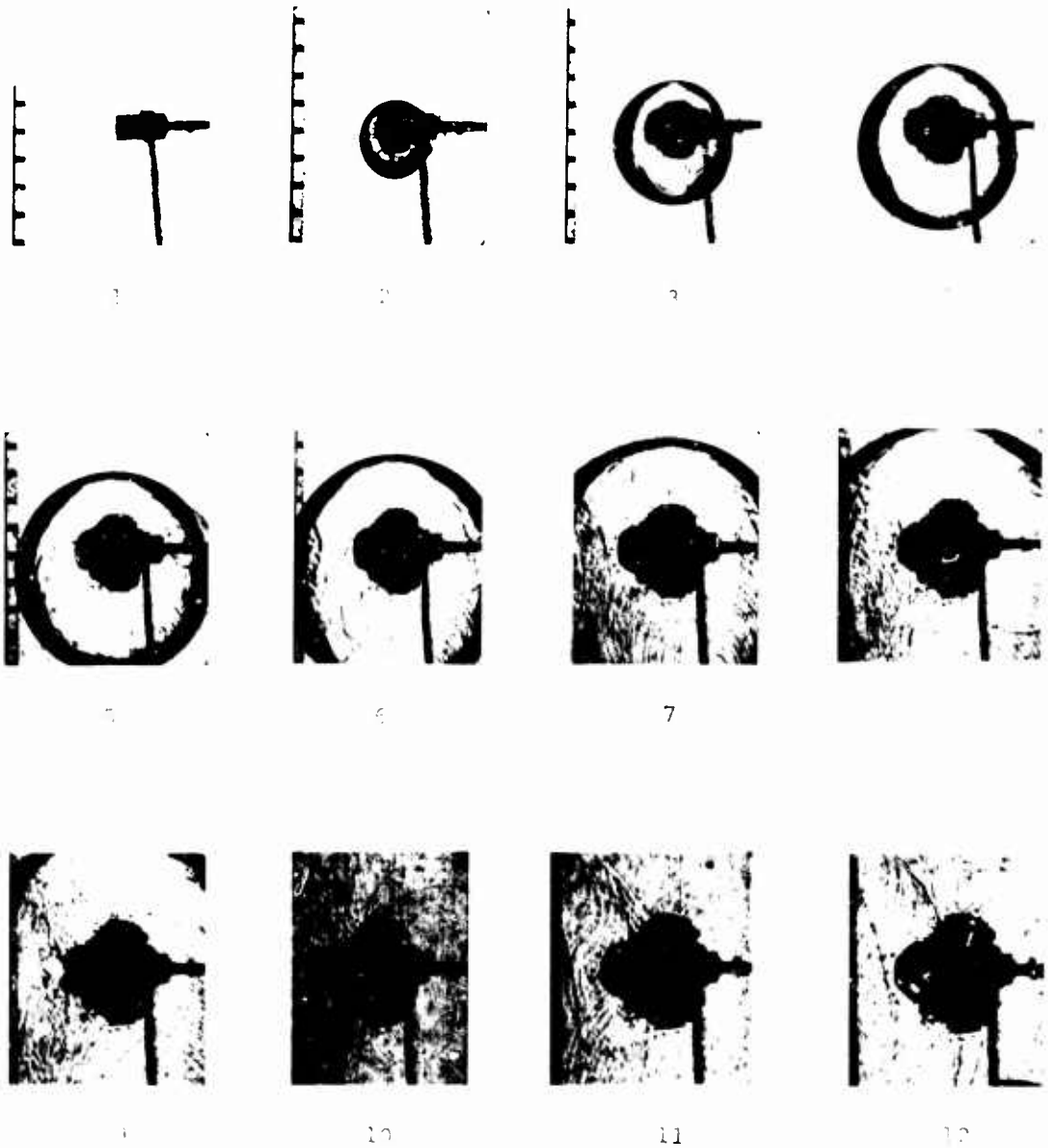


FIG. 10 FRAMING CAMERA SHADOWGRAPHS OF SHOCK WAVE AND PRODUCT GAS EXPANSION FROM THE M84 DETONATOR FIRED UNDERWATER

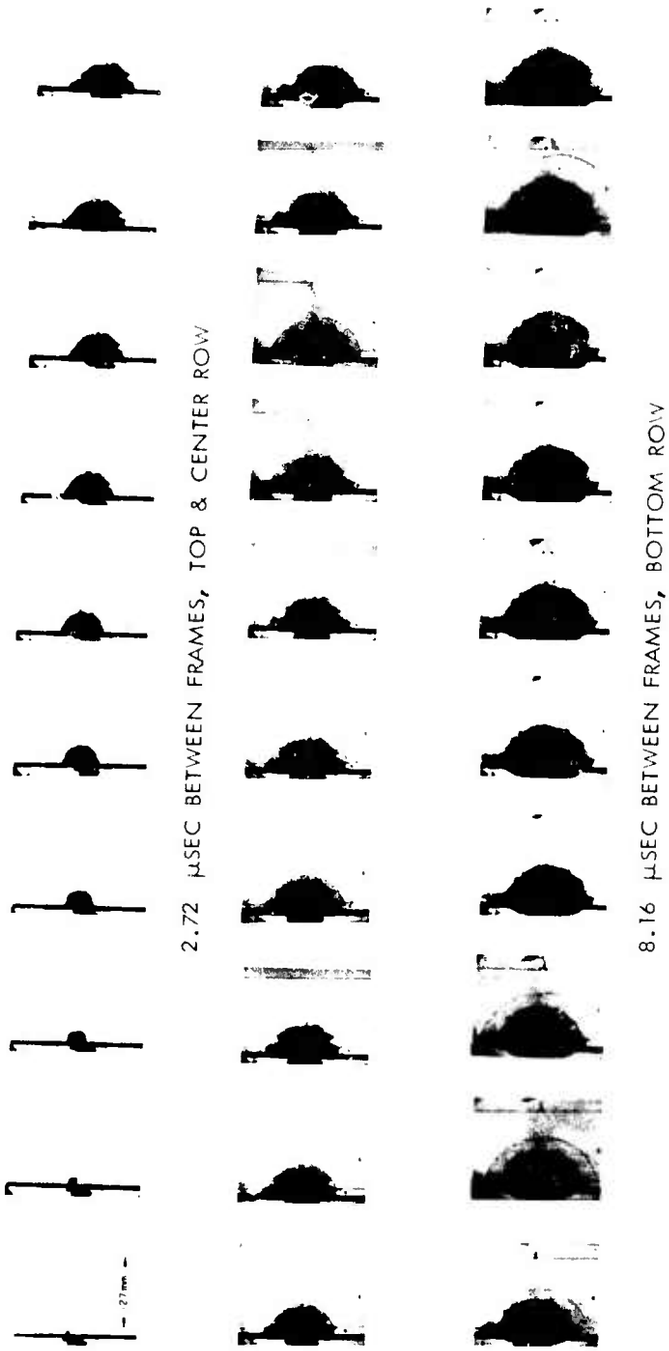


FIG. 11 FRAMING CAMERA SHADOWGRAPHS OF SHOCK WAVE EXPANSION FROM THE M84 DETONATOR FIRED IN AIR

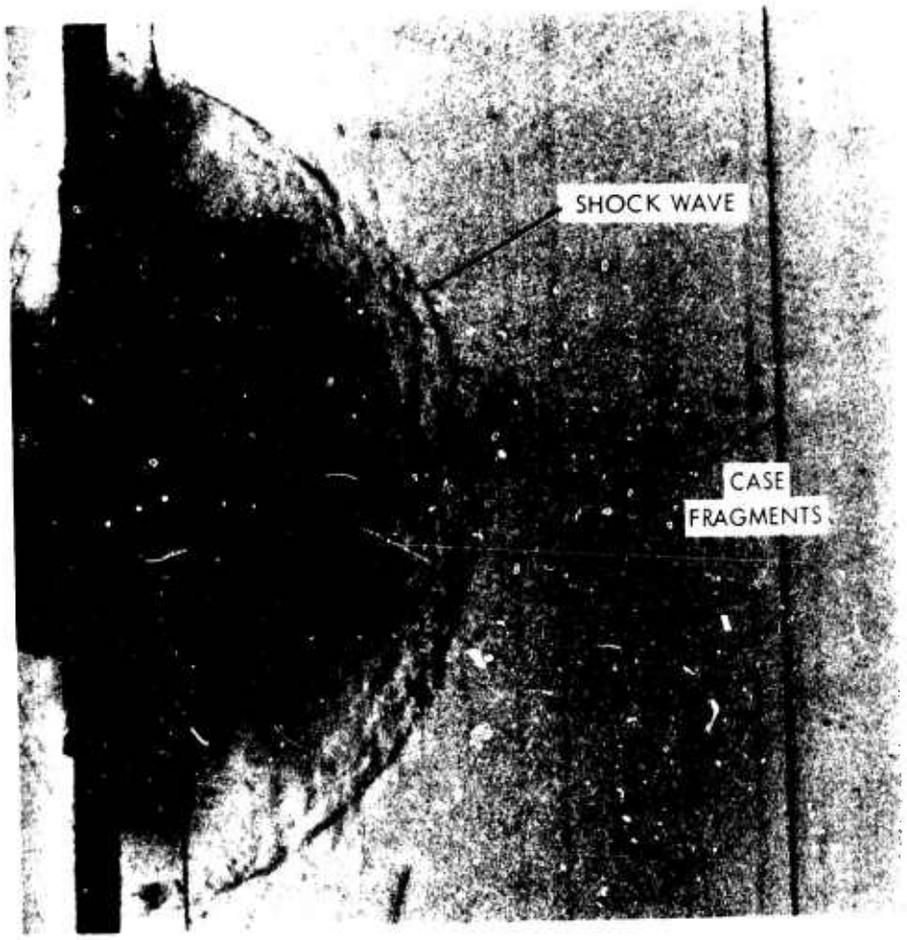


FIG. 11A AN ENLARGED FRAME FROM FIGURE 11

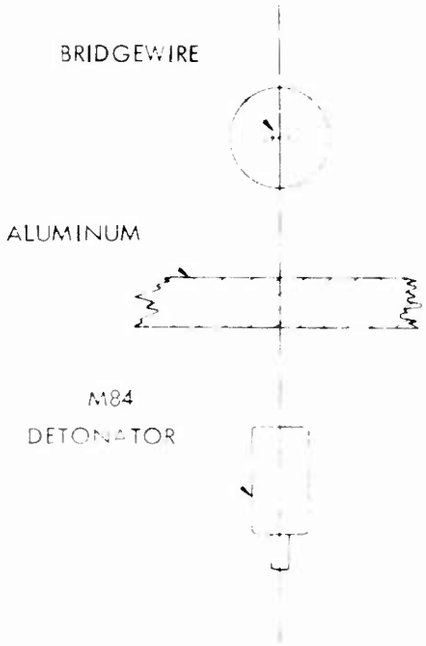


A.

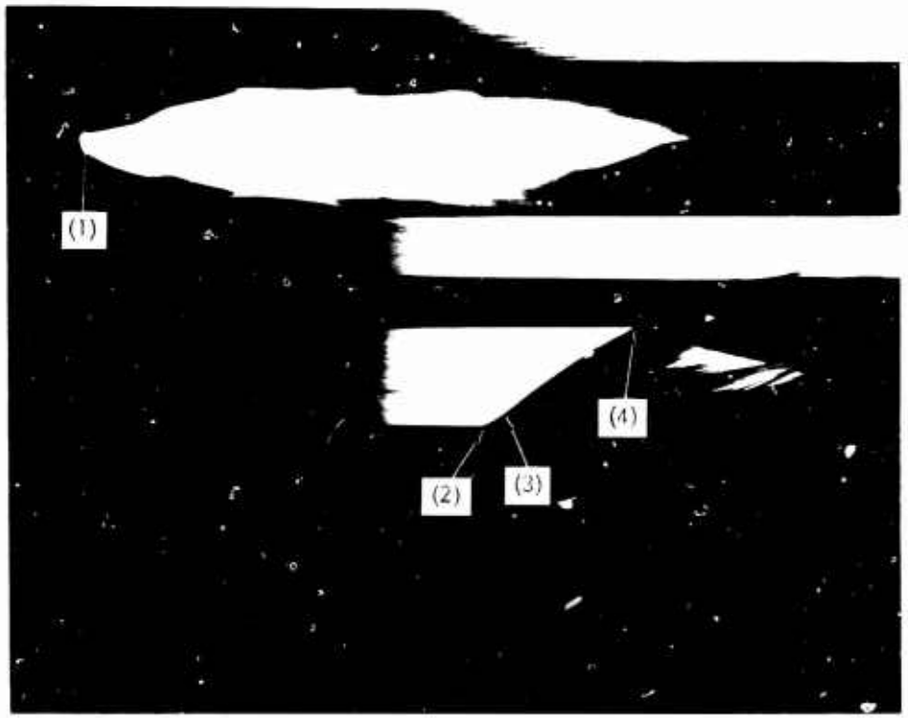


14 MICROSEC

B.

FIG. 12 A. TEST ARRANGEMENT
B. SMEAR CAMERA TRACE OF AXIAL SHOCK FROM THE M84 DETONATOR FIRED IN AIR (SEE PAGE 7 FOR EXPLANATION OF NUMBERS 1 - 4.)

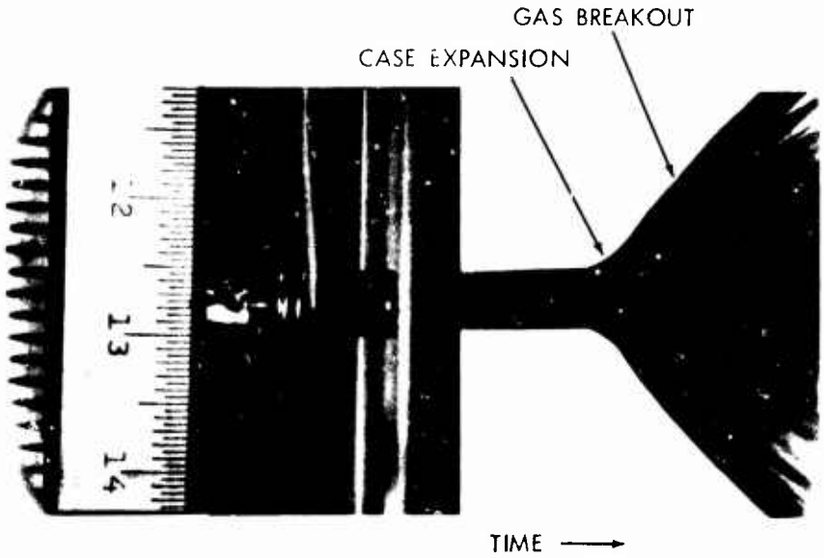


FIG. 13 SMEAR CAMERA RECORD OF LATERAL CASE EXPANSION FROM THE M84 DETONATOR FIRED IN AIR

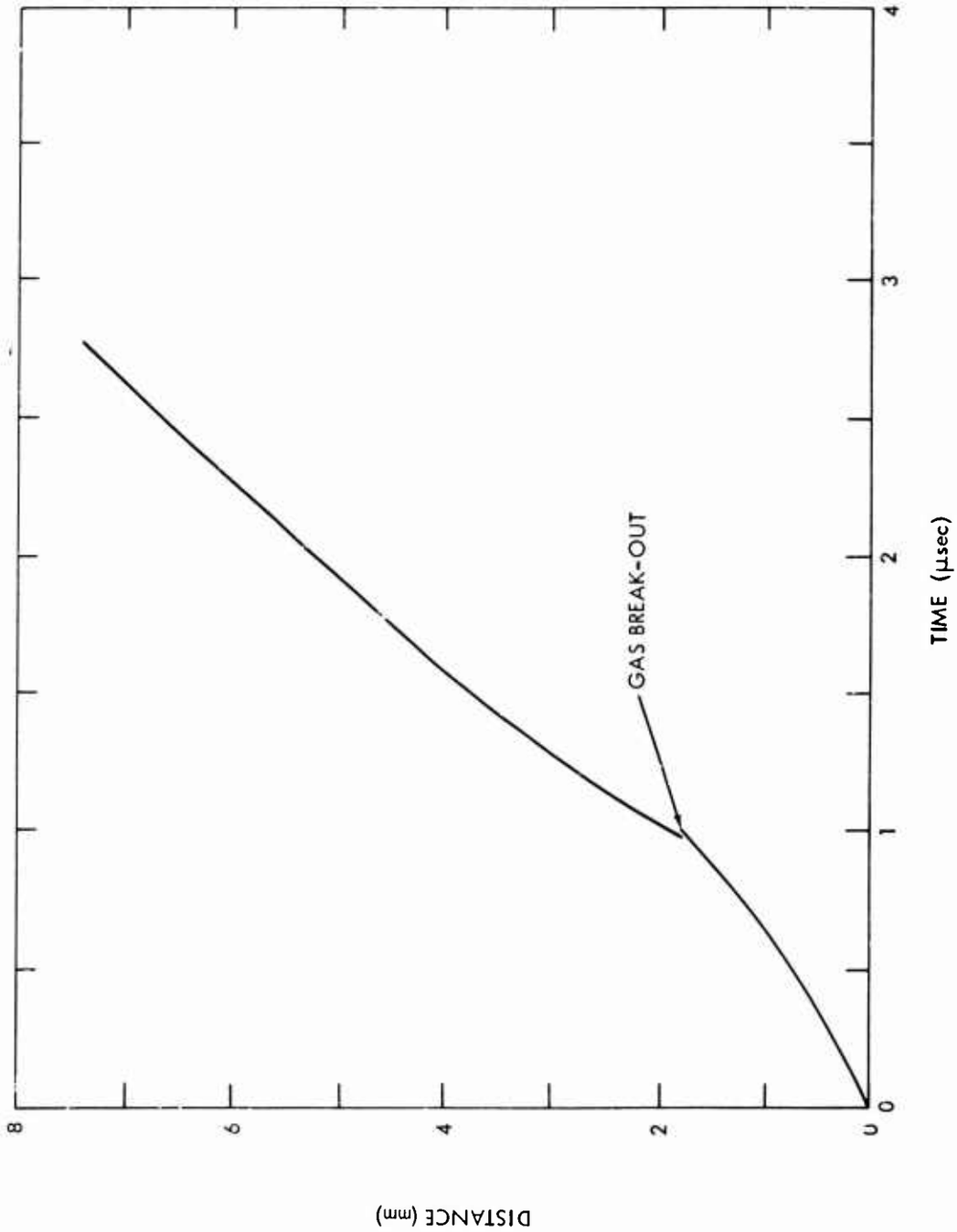


FIG. 14 CASE EXPANSION PROFILE FROM THE M84 DETONATOR FIRED IN AIR

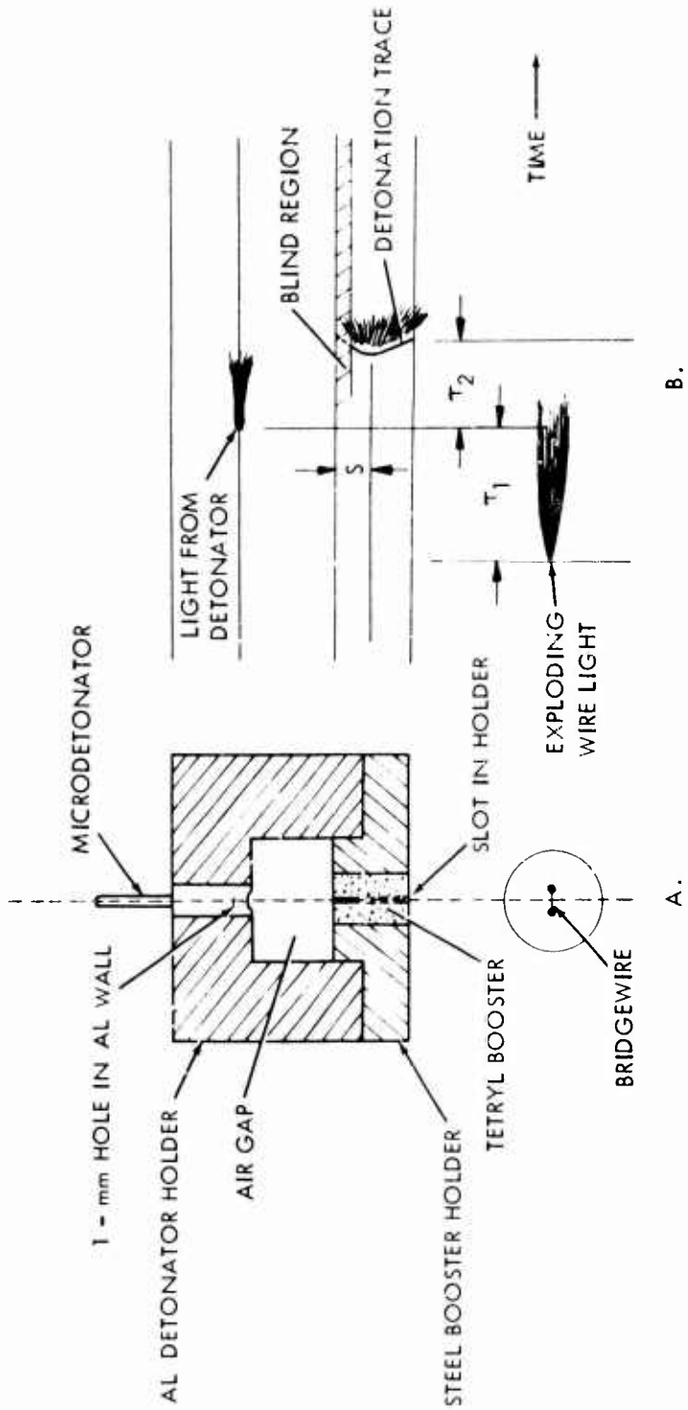


FIG. 15 A. THE MICRODETONATOR/TETRYL-BOOSTER SYSTEM

B. THE SMEAR-CAMERA TRACE OF THE DETONATION ALONG THE BOOSTER SURFACE AND THE STREAKS (TIMING MARKERS) FROM THE EXPLODING BRIDGEWIRE AND THE DETONATOR

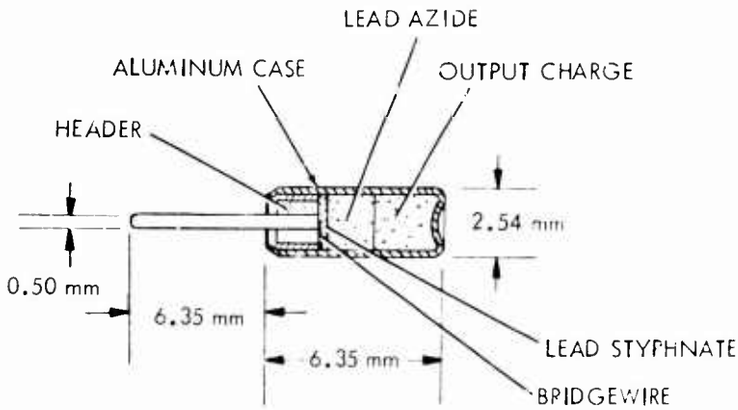


FIG. 16 THE MICRODETONATOR

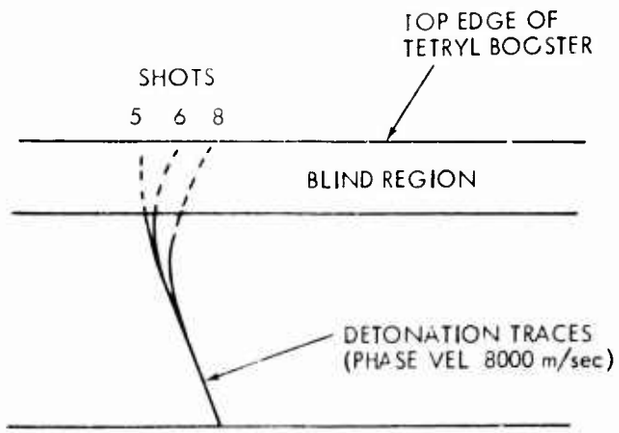


FIG. 17 SUPERPOSED SKETCHES OF THE DETONATION TRACES FROM SHOTS 5, 6, AND 8